

Supplementary Information for

Triboelectric nanogenerator with synergistic complementary nanopatterns by block copolymer self-assembly

*Seong-Yun Yun^{a,†}, Min Hyeok Kim^{b,†}, Geon Gug Yang^b, Hee Jae Choi^b, Do-Wan Kim^a, Yang-
Kyu Choi^{a,c,*}, and Sang Ouk Kim^{b,c,*}*

^a School of Electrical Engineering, Korea Advanced Institute of Science and Technology (KAIST), 291 Daehak-ro, Yuseong-gu, Daejeon 34141, Republic of Korea

^b National Creative Research Initiative Center for Multi-dimensional Directed Nanoscale Assembly, Department of Materials Science and Engineering, KAIST, 291 Daehak-ro, Yuseong-gu, Daejeon 34141, Republic of Korea

^c KAIST Institute for Nanocentury, KAIST, 291 Daehak-ro, Yuseong-gu, Daejeon 34141, Republic of Korea

†These authors equally contributed to this work.

* Address correspondence to ykchoi@ee.kaist.ac.kr

* Address correspondence to sangouk@kaist.ac.kr

1. Fabrication procedure of nanopatterns with BCP self-assembly

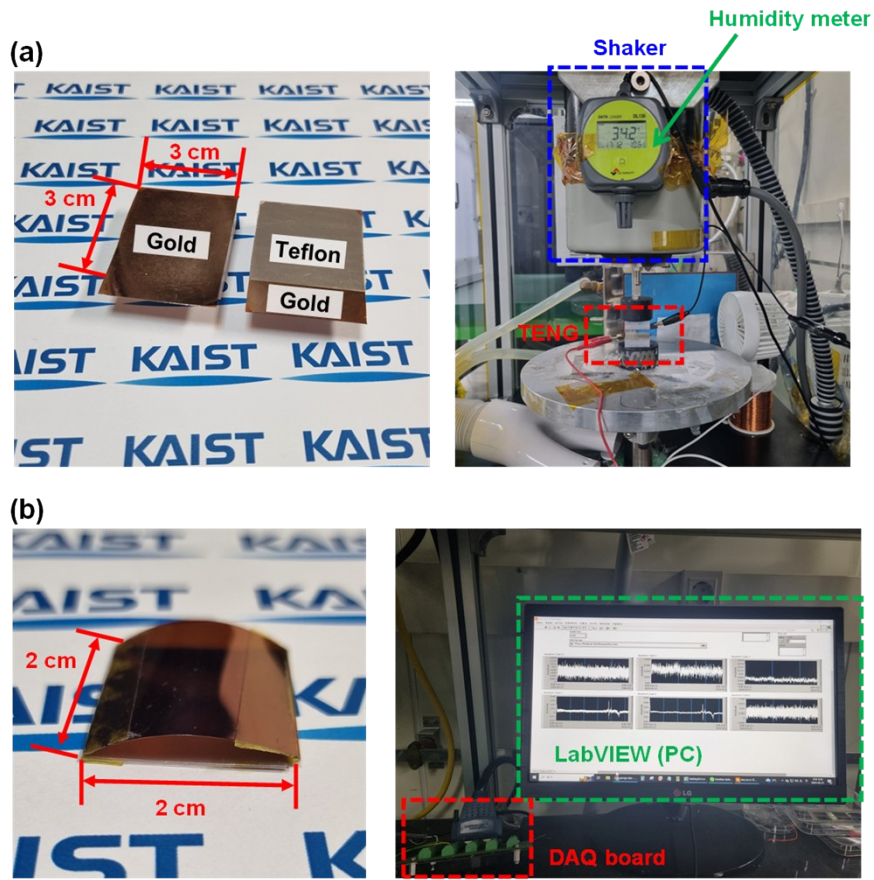


Figure S1. (a) Photographs of the CN-TENG and corresponding experimental bench to evaluate performances of prototyped CN-TENG. (b) Photographs of the CN-TENG and corresponding experimental bench for gait analyses.

2. Fabrication procedure of nanopatterns with BCP self-assembly

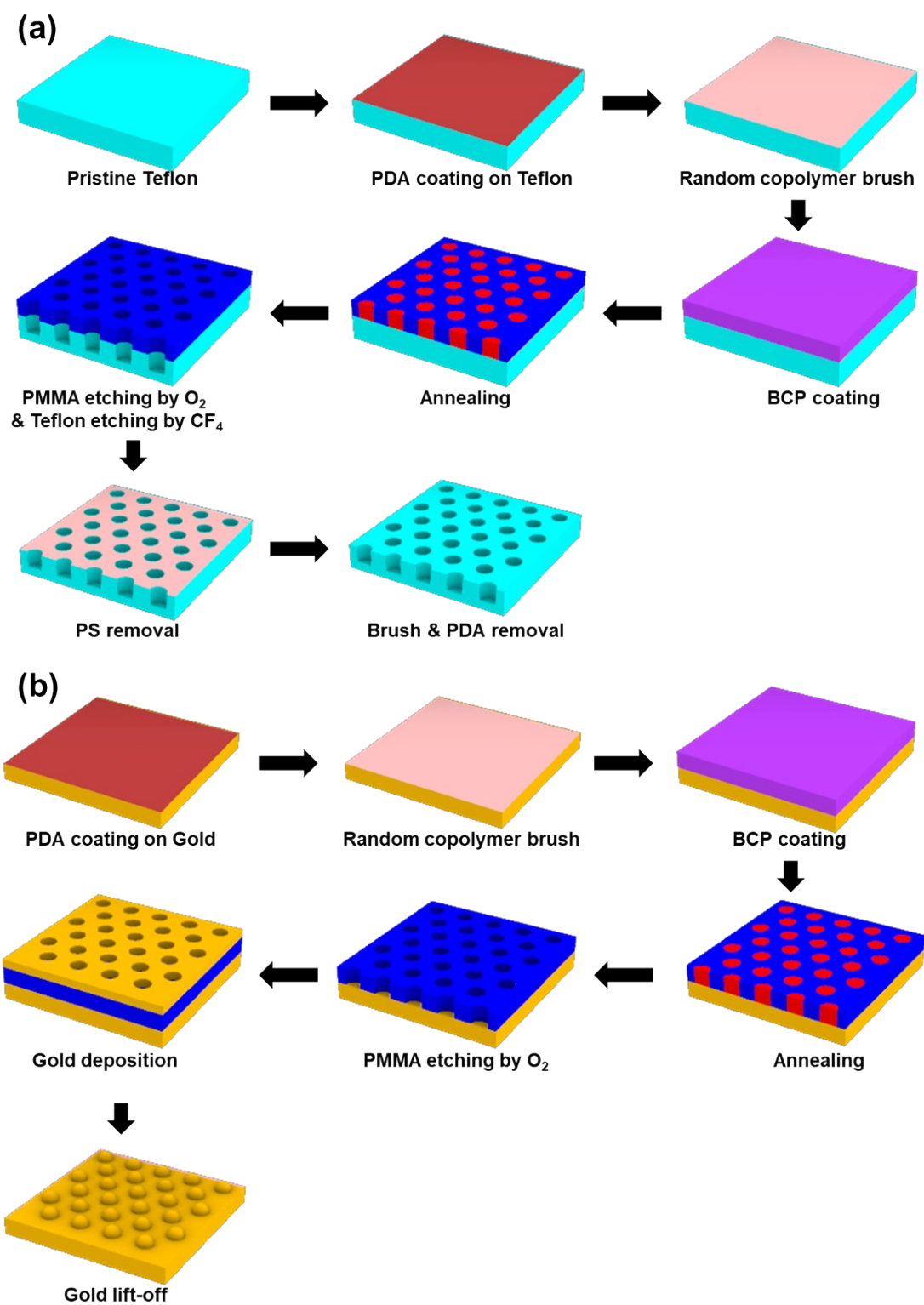


Figure S2. Detailed fabrication procedure to make nanopatterns with BCP self-assembly. (a)

Indented nanopores on Teflon. (b) Protruded nanodots on gold.

3. 6-inch wafer-scale fabrication of BCP



Figure S3. Fabricated BCP on a 6-inch Si wafer. By using BCP self-assembly, nanopatterns could be fabricated in wafer-scale.

4. Fast Fourier transform (FFT) images for various nanopatterns

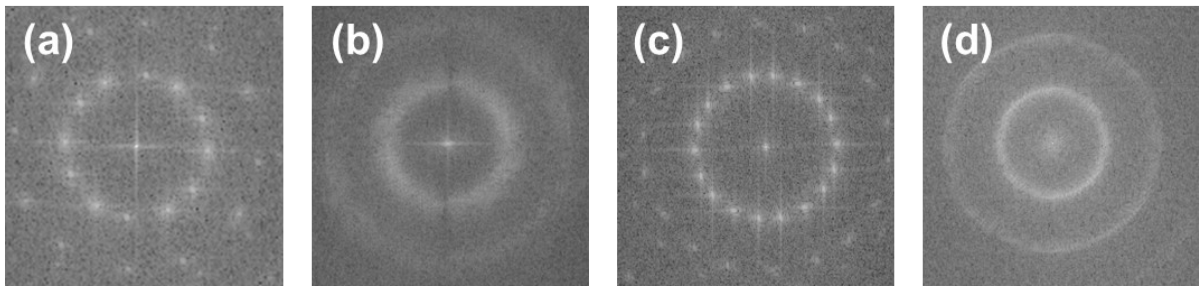


Figure S4. FFT analysis of nanopatterns. (a) Indented nanopores on Teflon and (b) indented nanotrenches on Teflon after PMMA etching with O_2 . (c) Protruded nanodots on gold and (d) protruded nanowires on gold after gold deposition and lift-off.

5. Intensity of grazing-incidence small-angle X-ray scattering (GISAXS) from nanopatterns

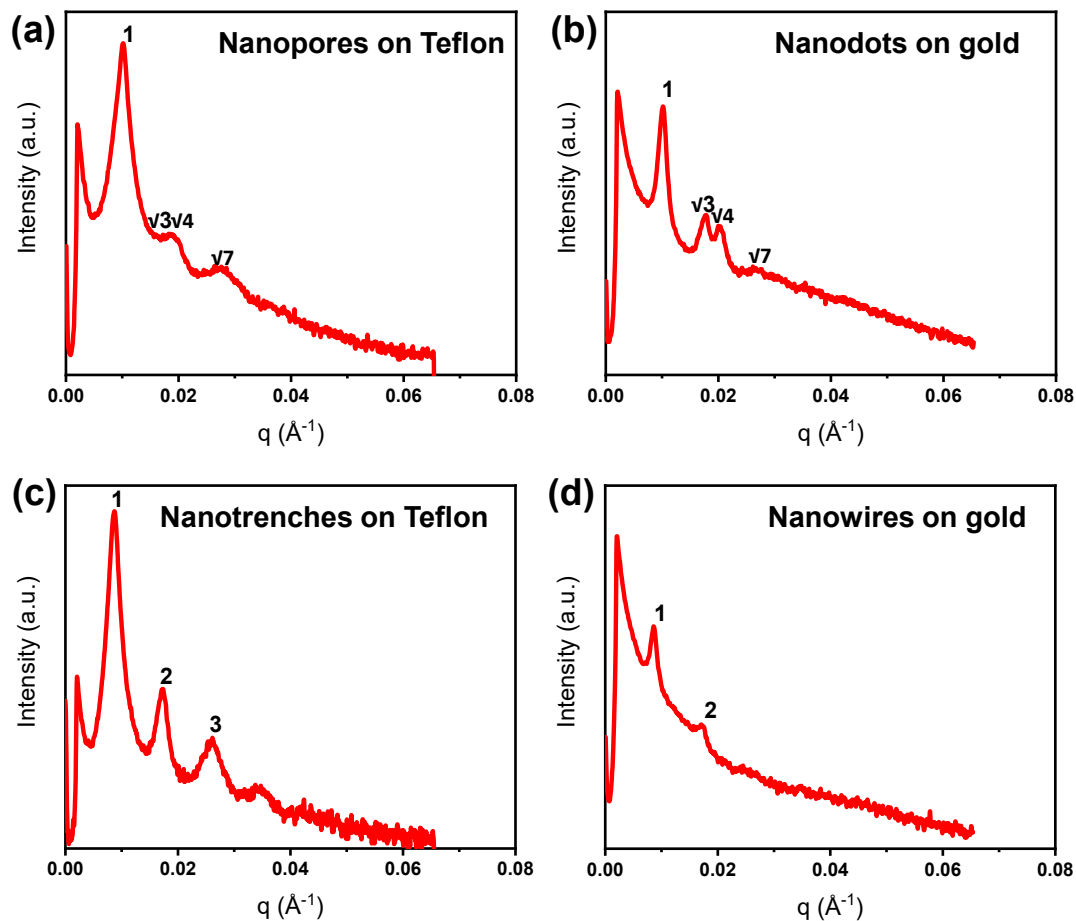


Figure S5. GISAXS intensity vs. q -plot for (a) indented nanopores on Teflon, (b) protruded nanodots on gold, (c) indented nanotrenches on Teflon, and (d) protruded nanowires on gold.

6. Analyses of nanopatterns on Teflon with X-ray photoelectron spectroscopy (XPS)

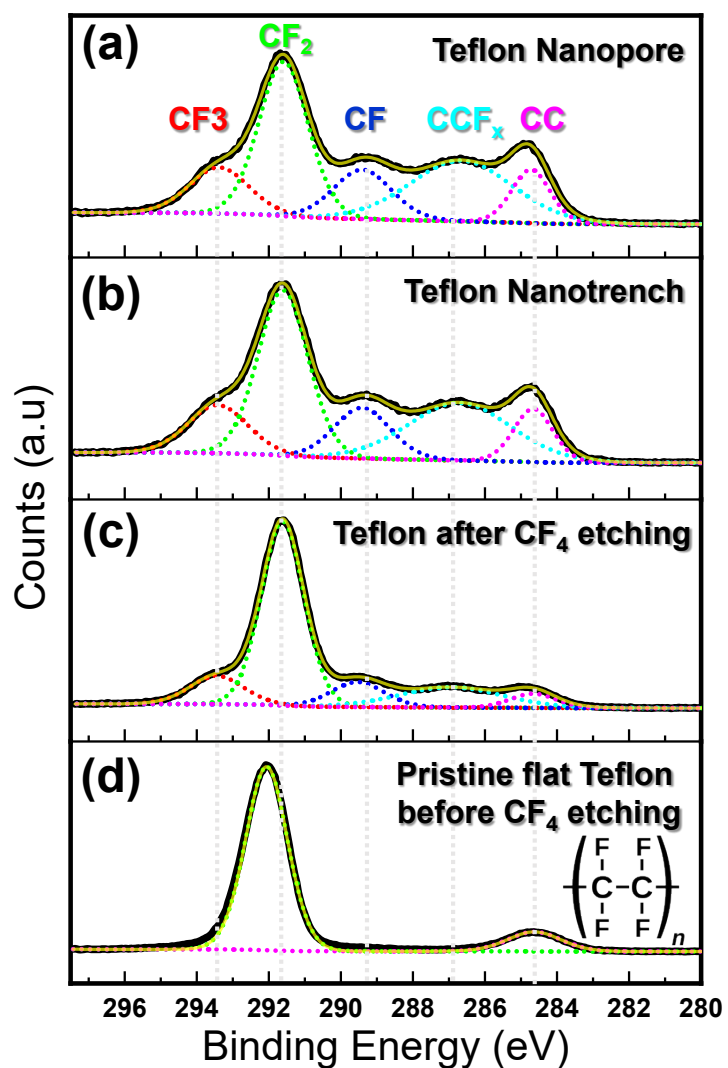


Figure S6. Energy spectra obtained from XPS for various nanopatterns. (a) Nanopores on Teflon. (b) Nanotrenches on Teflon. (c) Etched Teflon after CF_4 etching. (d) Pristine flat Teflon before CF_4 etching.

7. The effect of etching on TENG performances

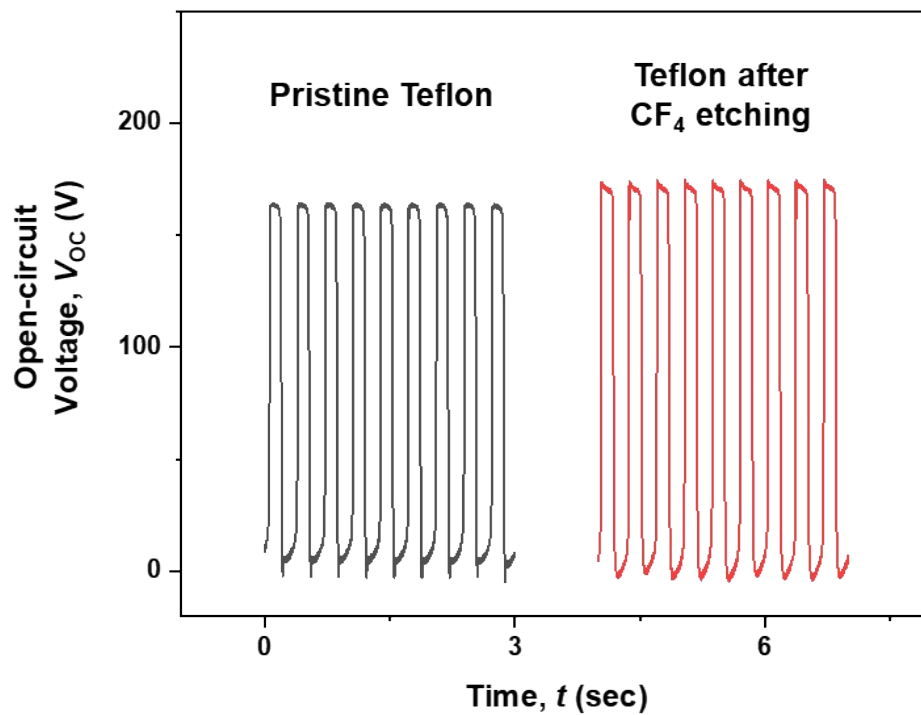


Figure S7. V_{OC} of TENGs with pristine smooth Teflon and roughened Teflon after CF_4 etching.

There was almost no difference between the two TENGs.

8. Measurement conditions for the TENG characterization

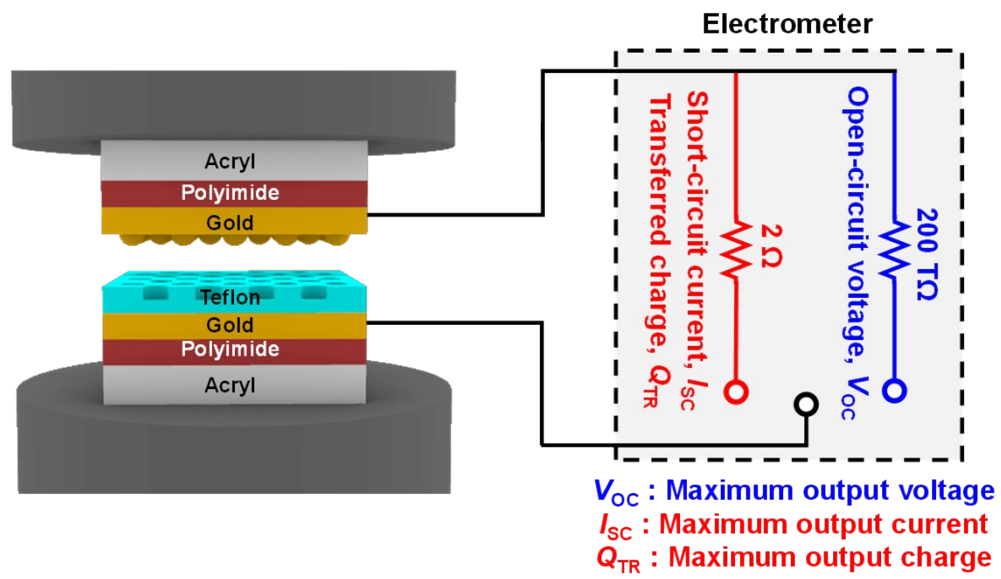
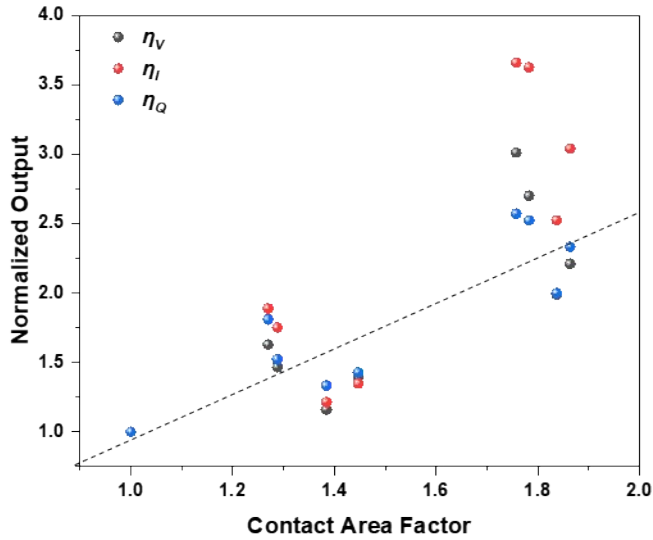


Figure S8. Measurement setup for characterization of TENGs.

9. Electrical output performances (η) according to contact area factor



$$\eta_V = \frac{V_{OC}(\text{Pattern})}{V_{OC}(\text{No Pattern})}$$

$$\eta_I = \frac{I_{SC}(\text{Pattern})}{I_{SC}(\text{No Pattern})}$$

$$\eta_Q = \frac{Q_{TR}(\text{Pattern})}{Q_{TR}(\text{No Pattern})}$$

Figure S9. Electrical output performances quantified as normalized output (η) according to the contact area factor. The normalized open-circuit voltage (η_V), short-circuit current (η_I), and transferred charge (η_Q) with pattern over those without pattern are defined by the equations above. The contact area factor was calculated as the product of the contact area increased due to the protrusion of the gold and the contact area increased due to the indentation of the Teflon.

10. Frequency effect on electrical outputs

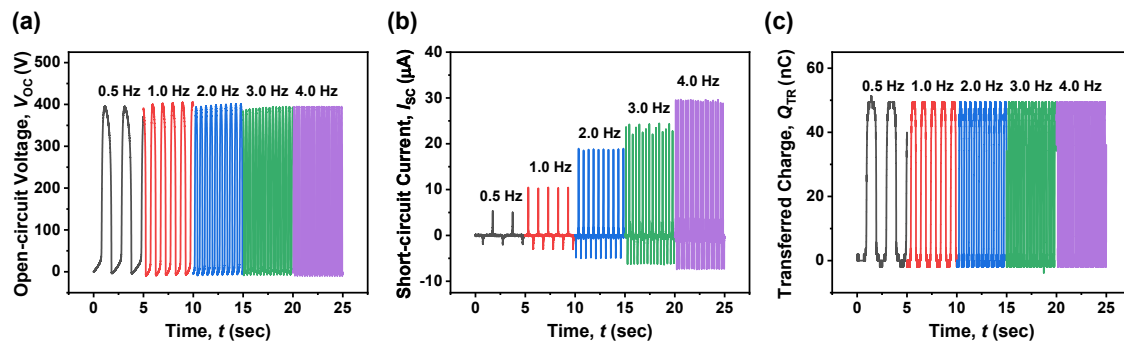


Figure S10. (a) Measured V_{OC} from the CN-TENGs with different frequencies from 0.5 Hz to 4.0 Hz. (b) Measured I_{SC} . (c) Measured Q_{TR} .

11. Demonstration of LED lighting with CN-TENG

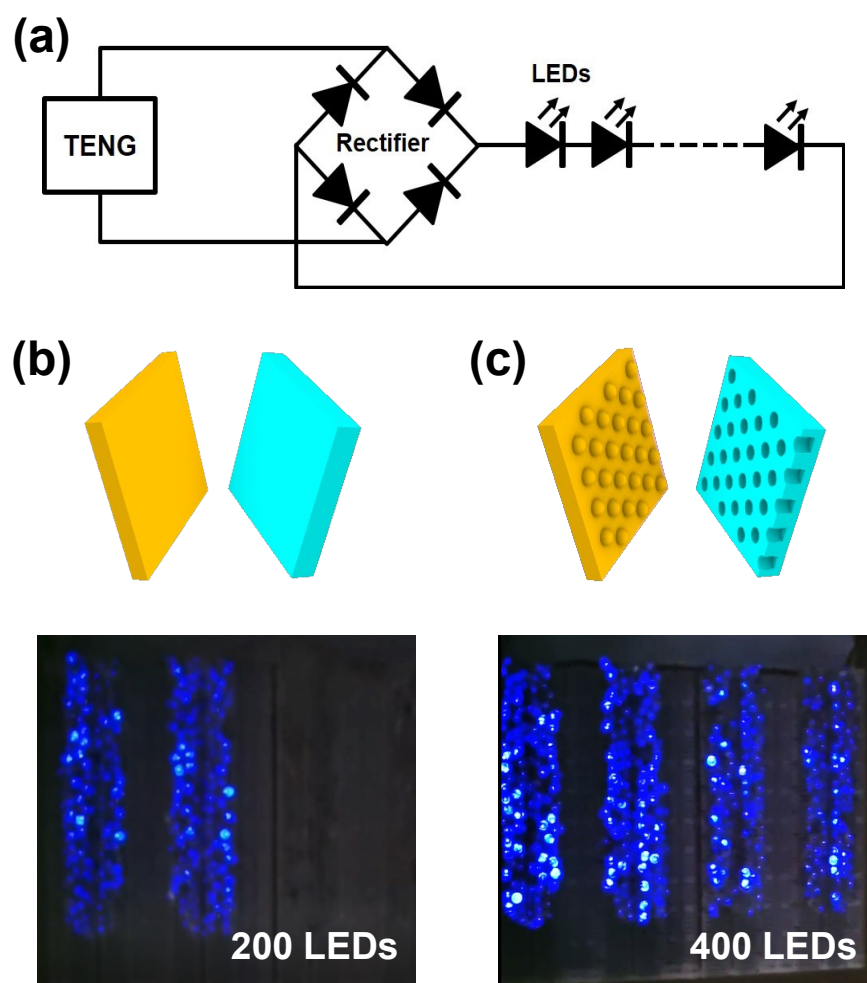


Figure S11. (a) Circuit diagram for LED lighting by CN-TENG. (b) Schematic illustration and optical photograph showing 200 illuminated LEDs by power generated from TENG without nanopatterns (No Pattern). (c) Schematic illustration and optical photograph showing 400 illuminated LEDs by power generated from CN-TENG with gold nanodots and Teflon nanopores (Pattern-6).

12. Size effect of complementary nanopatterns on electrical outputs

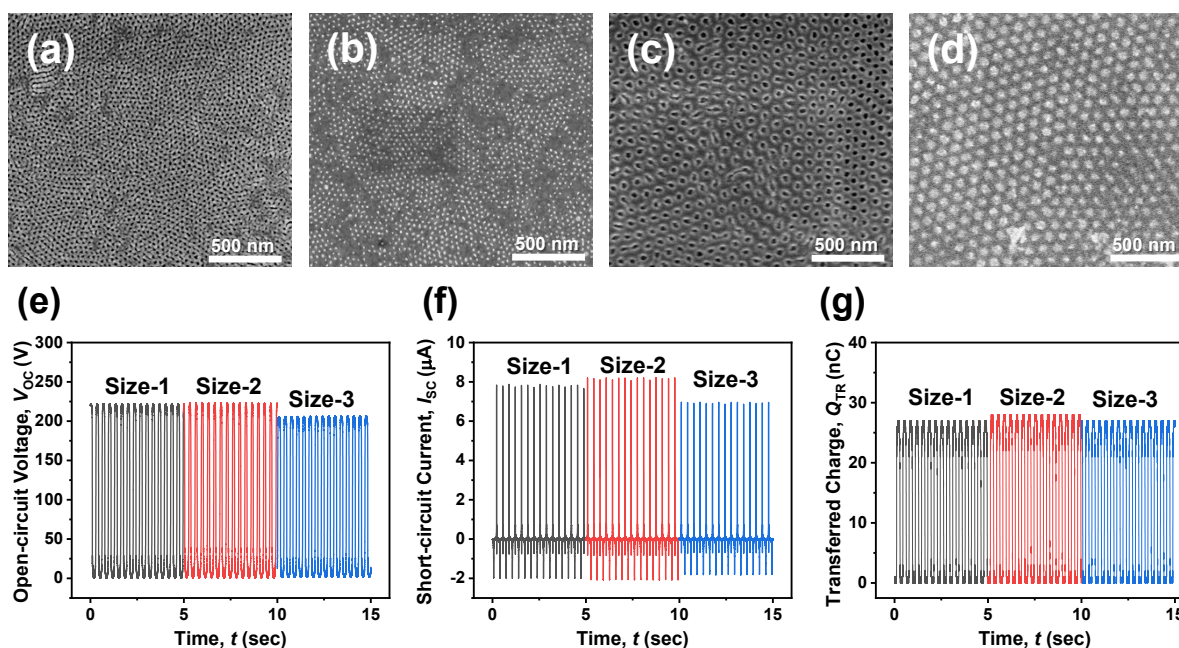


Figure S12. (a) SEM image of Tefflon nanopores fabricated by BCP with PS of 46.1 kg/mol and PMMA of 21 kg/mol (Size-1). (b) SEM image of gold nanodots fabricated by BCP with PS of 46.1 kg/mol and PMMA of 21 kg/mol (Size-1). (c) SEM image of Tefflon nanopores fabricated by BCP with PS of 328 kg/mol and PMMA of 173 kg/mol (Size-3). (d) SEM image of gold nanodots fabricated by BCP with PS of 328 kg/mol and PMMA of 173 kg/mol (Size-3). (e) Measured V_{OC} from the CN-TENGs with Size-1 to Size 3 listed in **Table S2**. (f) Measured I_{SC} . (g) Measured Q_{TR} .

13. Classification accuracy according to the number of epochs

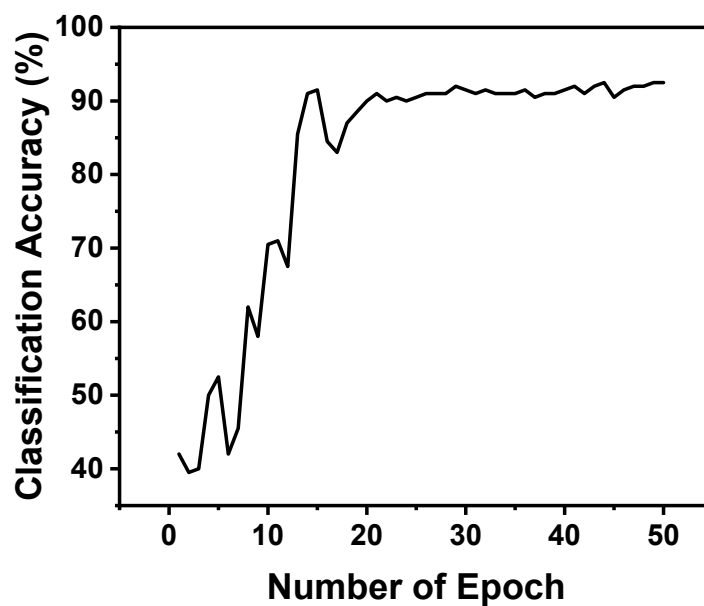


Figure S13. Classification accuracy as a function of the number of training epochs.

Table S1. Various CN-TENGs and TENGs of 9 combinatorial pattern-pairs among flat gold, gold nanodots, gold nanowires, flat Teflon, Teflon nanopores, and Teflon nanotrenches. For gold nanodots and Teflon nanopores, PS with M_w of 132 kg/mol and PMMA with M_w of 68 kg/mol were used. For gold nanowires and Teflon nanotrenches, PS with M_w of 105 kg/mol and PMMA with M_w of 106 kg/mol were used.

TENG Type	Gold	Teflon	Remark
No Pattern	Flat (without pattern)	Flat (without pattern)	TENG with both flat surfaces
Pattern-1	Nanowires	Flat (without pattern)	TENG with rough surface on single-side
Pattern-2	Nanodots	Flat (without pattern)	
Pattern-3	Flat (without pattern)	Nanopores	
Pattern-4	Flat (without pattern)	Nanotrenches	
Pattern-5	Nanowires	Nanopores	CN-TENG with rough surface on double-sides
Pattern-6	Nanodots	Nanopores	
Pattern-7	Nanowires	Nanotrenches	
Pattern-8	Nanodots	Nanotrenches	

Table S2. Various CN-TENGs of 3 combinatorial size-pairs between gold nanodots and Teflon nanopores. To control a size of a gold nanodot and a Teflon nanopore, various M_w of PS and PMMA were used.

TENG Type	Gold nanodot (M_w of PS : M_w of PMMA) [kg/mol]	Teflon nanopore (M_w of PS : M_w of PMMA) [kg/mol]	Remark
Size-1	46.1 : 21	46.1 : 21	Small
Size-2	132 : 68	132 : 68	Medium
Size-3	328 : 173	328 : 173	Large